

Hyperon-nucleon scattering and hyperon masses in the nuclear medium

C. L. Korpa

Department of Theoretical Physics, University of Pecs, Ifjusag u. 6, H-7624 Pecs, Hungary

A. E. L. Dieperink and R. G. E. Timmermans

Kernfysisch Versneller Instituut, Zernikelaan 25, NL-9747AA Groningen, The Netherlands

(Received 20 July 2001; published 18 December 2001)

We analyze low-energy hyperon-nucleon scattering using an effective field theory in next-to-leading order. By fitting experimental cross sections for laboratory hyperon momenta below 200 MeV/c and using information from the hypertriton we determine 12 contact-interaction coefficients. Based on these we discuss the low-density expansion of hyperon mass shifts in the nuclear medium.

DOI: 10.1103/PhysRevC.65.015208

PACS number(s): 13.75.Ev, 14.20.-c, 21.30.Fe

I. INTRODUCTION

The binding energy of hyperons in nuclear matter plays an important role in hypernuclei and in the equation of state of neutron stars. The most commonly used approach is that one starts from a two-body hyperon-nucleon potential based upon one-boson exchange (OBE) and SU(3)-flavor symmetry and then computes the binding of hyperons in matter in the Brueckner approximation. It has been shown that uncertainties in the two-body input may lead to large differences in the resulting hyperon potentials and in particular in the binding of the sigma hyperons [1]. Therefore it is appropriate to see whether other approaches, e.g., a low-density expansion based on vacuum scattering amplitudes can provide additional insight.

Alternatively, Savage and Wise [2] have analyzed hyperon mass shifts in nuclear matter using chiral perturbation theory by expanding in the Fermi momentum. The interactions were determined by a chiral Lagrangian with SU(3) \times SU(3) symmetry; the hyperon mass shifts could be expressed in terms of six coefficients related to the strength of the four-baryon contact interactions and the pseudoscalar-meson couplings to baryons and were computed at the one-loop level. However, the unknown values of these six parameters prevented them from obtaining numerical results for the energy shift at zero momentum.

More recently, applications of effective field theory (EFT) in nuclear physics have received a renewed interest (for a review see Refs. [3,4]). So far, most investigations have been devoted to the two-nucleon system, which is characterized by anomalously large scattering lengths. The existence of quasibound states introduces an additional scale in the problem, complicating the power counting required in EFT. A remedy was recently proposed [5–8] in the form of a selective resummation. The leading-order amplitude of this approach reproduces the effective-range expansion with a vanishing range parameter [8]. Inclusion of the next-to-leading order terms produces a nonzero effective range.

It is tempting to study whether a similar approach can be applied to the hyperon-nucleon sector which involves coupled channels, i.e., the scattering length and the effective range are represented by matrices. Since our region of application (center-of-mass momenta below 100 MeV/c) is be-

low the pion cut, and in view of the problems [9] encountered with perturbative pions [5], we use an approach without explicit mesons. Thus the two-baryon interaction to leading order involves six constant contact terms, since SU(3) \times SU(3) can be decomposed into the sum of six irreducible representations of SU(3). For the *s* waves we consider, the next-to-leading (NLO) order introduces six additional SU(3)-symmetry respecting coefficients for the terms of order p^2 . The absence of experimental information on ΞN scattering means that the low-energy hyperon-nucleon data in the present approach depend only on ten (out of these 12) parameters.

As discussed in the following sections, breaking of SU(3) symmetry by meson masses has significant consequences. We model this symmetry breaking by incorporating terms of order p^2 coming from one-pion exchange. The two coefficients of these terms we treat as free parameters, resulting in a total of 12 parameters.

In Sec. II we formulate the coupled-channels formalism, based on effective field theory, for low-energy hyperon-nucleon scattering. In Sec. III we present results of the fit to *YN* cross sections and ΛN scattering lengths. Some information on the latter is provided by the calculation of the hypertriton binding energy [10]. Results for the hyperon mass shifts in low-density nuclear medium and their comparison to results obtained by other methods are presented in Sec. IV.

II. HYPERON-NUCLEON SCATTERING

We consider hyperon-nucleon scattering at low energy and use the approach of effective field theory. In general the tree-level amplitude in next-to-leading order is written as

$$\mathcal{A}_0 = -C_0 - C_2 p^2, \quad (1)$$

where C_0 and C_2 denote matrices whose elements are the relevant coefficients in the interaction Lagrangian.

The Kaplan-Savage-Wise (KSW) resummation [5,8] gives, in leading order, a scattering amplitude \mathcal{A} given by

$$\mathcal{A}^{-1} = \mathcal{A}_0^{-1} - \frac{M_r}{2\pi} (\mu + ip), \quad (2)$$

with M_r , the reduced baryon mass (for which we take a common value in all channels) and μ the (arbitrary) subtraction point. Using the relation between the K matrix and the full amplitude \mathcal{A} , viz.

$$pK^{-1} = \frac{2\pi}{M_r} \mathcal{A}^{-1} + ip, \quad (3)$$

we obtain for the KSW resummation

$$pK^{-1} = -\mu - \frac{2\pi}{M_r} (C_0 + C_2 p^2)^{-1}. \quad (4)$$

By expanding the term $(C_0 + C_2 p^2)^{-1}$ in powers of p^2 we recover the effective-range expansion

$$pK^{-1} = -\frac{1}{a} + \frac{1}{2} r p^2 + \dots, \quad (5)$$

where the scattering-length matrix a and effective-range matrix r are given by

$$a^{-1} = \mu + \frac{2\pi}{M_r} C_0^{-1}, \quad (6)$$

$$r = \frac{4\pi}{M_r} C_0^{-1} C_2 C_0^{-1}. \quad (7)$$

To accommodate possibly large values of the scattering length in the momentum expansion of the amplitude one should keep all powers of ap . This leads to the following expression for the amplitude in NLO:

$$\begin{aligned} \mathcal{A} = & -\frac{2\pi}{M_r} \left(\mu + ip + \frac{2\pi}{M_r} C_0^{-1} \right)^{-1} \left[1 + \frac{2\pi p^2}{M_r} C_0^{-1} C_2 C_0^{-1} \right. \\ & \left. \times \left(\mu + ip + \frac{2\pi}{M_r} C_0^{-1} \right)^{-1} \right]. \end{aligned} \quad (8)$$

This is a generalization of the single-channel expression, see Eq. (2.18) in Ref. [5], to coupled channels.

Next we turn to the relationship between elements of the tree-level amplitude matrix C_0 , corresponding to the two-baryon scattering amplitudes of interest. For the spin-1/2 baryon octet it is convenient to express the six real parameters determining the constant four-baryon contact interactions through coefficients corresponding to the six irreducible representations of the direct product $SU(3) \times SU(3)$, which is appropriate for baryon-baryon scattering. We write the coefficients of the terms in the Lagrangian for $B_1 B_2 \rightarrow B_3 B_4$ in the form $-b_S(B_1 B_2 \rightarrow B_3 B_4)/f^2$, where $f \approx 132$ MeV can be identified with the pion decay constant and $S=0$ or 1 denotes the total spin. Introducing the notation $s_0, s_1, s_2, t_1, t_2, t_3$ for the coefficients of the representations [1], [27], $[8_s]$, [10], [10], $[8_a]$, respectively, we list the b_S values of interest (we note that some of them are given in Ref. [11]) below.

(i) For the single-channel case $\Sigma^+ p \rightarrow \Sigma^+ p$:

$$b_0(\Sigma^+ p \rightarrow \Sigma^+ p) = s_1, \quad b_1(\Sigma^+ p \rightarrow \Sigma^+ p) = t_2. \quad (9)$$

(ii) For coupled channels $\Sigma^+ n$, $\Sigma^0 p$, and Λp :

$$b_0(\Sigma^+ n \rightarrow \Sigma^+ n) = \frac{1}{5}(2s_1 + 3s_2),$$

$$b_0(\Sigma^0 p \rightarrow \Sigma^0 p) = \frac{1}{10}(7s_1 + 3s_2),$$

$$b_0(\Lambda p \rightarrow \Lambda p) = \frac{1}{10}(9s_1 + s_2),$$

$$b_0(\Sigma^+ n \rightarrow \Sigma^0 p) = \frac{3\sqrt{2}}{10}(s_1 - s_2),$$

$$b_0(\Sigma^+ n \rightarrow \Lambda p) = -\frac{\sqrt{6}}{10}(s_1 - s_2),$$

$$C_0(\Sigma^0 p \rightarrow \Lambda p) = \frac{\sqrt{3}}{10}(s_1 - s_2),$$

$$b_1(\Sigma^+ n \rightarrow \Sigma^+ n) = \frac{1}{3}(t_1 + t_2 + t_3),$$

$$b_1(\Sigma^0 p \rightarrow \Sigma^0 p) = \frac{1}{6}(t_1 + 4t_2 + t_3),$$

$$b_1(\Lambda p \rightarrow \Lambda p) = \frac{1}{2}(t_1 + t_3),$$

$$b_1(\Sigma^+ n \rightarrow \Sigma^0 p) = -\frac{\sqrt{2}}{6}(t_1 - 2t_2 + t_3),$$

$$b_1(\Sigma^+ n \rightarrow \Lambda p) = \frac{1}{\sqrt{6}}(t_1 - t_3),$$

$$b_1(\Sigma^0 p \rightarrow \Lambda p) = \frac{\sqrt{3}}{6}(-t_1 + t_3). \quad (10)$$

We mention that coupling between above channels has been neglected in Ref. [2].

(iii) Similarly there is coupling between channels containing $\Sigma^- p$, $\Sigma^0 n$, and Λn , with coefficients equal to those given in Eq. (10), except for an overall sign change for $b_S(\Sigma^- p \rightarrow \Lambda n)$ and $b_S(\Sigma^0 n \rightarrow \Lambda n)$, compared to $b_S(\Sigma^+ n \rightarrow \Lambda p)$ and $b_S(\Sigma^0 p \rightarrow \Lambda p)$. All coefficients b_S are subtraction-point dependent.

The coefficients of the p^2 term C_2 in Eq. (4), which we denote by $s'_1, s'_2, t'_1, t'_2, t'_3$ (apart from the common factor $1/f^4$ to make these coefficients dimensionless), obey the same relationships as in Eq. (10), since the latter are valid for the full momentum-dependent s-wave amplitudes [11]. Hence they are valid for the momentum expansion terms and also for tree-level amplitudes, since the loop expansion corresponds to an expansion in powers of \hbar .

Let us briefly discuss the breaking of the $SU(3)$ -flavor symmetry [keeping $SU(2)$ -isospin symmetry]. In a study of

its significance it is concluded [11] that, apart from consequences of the pseudoscalar-meson mass differences and the baryon mass differences the SU(3) symmetry is satisfied quite well. The differences in baryon masses we take explicitly into account. The symmetry breaking due to different meson masses is modeled by considering one-pion exchange (i.e., ignoring the kaon and the eta). To be consistent with the above NLO approach without mesons, we expand the exchange amplitude and keep only the leading, order p^2 , term. This basically leads to addition of a symmetry-breaking term $-C_2'p^2/f^4$ to tree-level amplitude, Eq. (1), depending on two parameters, u_1 and u_2 . The relevant coefficients in the spin-singlet channel are the following:

$$C_2'(\Sigma^+n \rightarrow \Sigma^+n) = 2u_1, \quad C_2'(\Sigma^+n \rightarrow \Sigma^0p) = -2\sqrt{2}u_1,$$

$$C_2'(\Sigma^+n \rightarrow \Lambda p) = 2\sqrt{2/3}u_2, \quad C_2'(\Sigma^0p \rightarrow \Lambda p) = \frac{2}{\sqrt{3}}u_2. \quad (11)$$

The spin-triplet coefficients are obtained by multiplying the above values with $-1/3$. For the channels Σ^-p , Σ^0n , and Λn the only difference is in the sign of the term $C_2'(\Sigma^0n \rightarrow \Lambda n)$ compared to $C_2'(\Sigma^0p \rightarrow \Lambda p)$.

III. APPLICATION TO HYPERON-NUCLEON SCATTERING DATA

We now turn to the available low-energy data on hyperon-nucleon scattering. We consider only scattering with laboratory momenta below 200 MeV/c, i.e., center-of-mass momenta less than 100 MeV/c. There is only a small amount of relevant data, corresponding to total cross sections for $\Sigma^+p \rightarrow \Sigma^+p$, $\Lambda p \rightarrow \Lambda p$, $\Sigma^-p \rightarrow \Sigma^-p$, $\Sigma^-p \rightarrow \Sigma^0n$ and $\Sigma^-p \rightarrow \Lambda n$ scattering (see, for example, Ref. [12]). It has been known for a long time [13] that these available data do not allow a unique effective-range analysis. The most precisely determined quantity is the ‘‘capture ratio at rest,’’

$$r_R = \frac{1}{4}r_0 + \frac{3}{4}r_1, \quad (12)$$

with

$$r_S = \frac{\sigma_S(\Sigma^-p \rightarrow \Sigma^0n)}{\sigma_S(\Sigma^-p \rightarrow \Sigma^0n) + \sigma_S(\Sigma^-p \rightarrow \Lambda n)}, \quad (13)$$

where the cross sections are taken at zero momentum and S denotes the total spin.

When fitting the calculated cross sections to the data we make two corrections, following Ref. [11]. First, the $\Sigma^-p \rightarrow \Lambda n$ transitions are kinematically suppressed relative to $\Sigma^-p \rightarrow \Sigma^0n$, as a consequence of the large momentum release, which at threshold is 290 MeV/c. According to Ref. [11] this necessitates inclusion of a correction factor $r_F \approx 0.16$ in the calculated cross section for $\Sigma^-p \rightarrow \Lambda n$. The second correction concerns the non-negligible contribution of the ${}^3S_1 \rightarrow {}^3D_1$ transition in the experimentally measured cross section $\sigma_1(\Sigma^-p \rightarrow \Lambda n)$. Defining the ratio r_{ds} of 3S_1

$\rightarrow {}^3D_1$ to ${}^3S_1 \rightarrow {}^3S_1$ cross sections for $\Sigma^-p \rightarrow \Lambda n$, a value of $r_{ds} \approx 0.57$ was estimated in Ref. [11].

We first attempted a fit of 28 data points (the cross sections shown in Fig. 1. and the capture ratio $r_R = 0.468 \pm 0.010$) with the leading-order calculation involving the 5 parameters s_1, s_2, t_1, t_2, t_3 , varying the value of the subtraction point μ . In this leading-order calculation we could not achieve a reasonable fit.

Then we turned to the next-to-leading-order computation, which added the five SU(3)-symmetry respecting parameters $s'_1, s'_2, t'_1, t'_2, t'_3$, as well as the two symmetry breaking ones, u_1 and u_2 . As further constraint we used the existence of the hypertriton bound state [10], which is compatible with the OBE potential NSC97f of Ref. [12]. The advantage of this [13] is that while the scattering data are mainly sensitive to the 3S_1 ΛN interaction, the hypertriton is more sensitive to the 1S_0 ΛN interaction. Thus we imposed as requirement on the fit that it had to lead to Λ -nucleon scattering lengths of $a_{\Lambda N}^{(0)} \approx -2.5$ fm for the singlet, and $a_{\Lambda N}^{(1)} \approx -1.75$ fm for the triplet state, respectively.

Several fits of the same quality, χ^2 being around 13 (for 16 degrees of freedom) could be obtained. If a fit was obtained for a certain value of the subtraction point μ , it is possible to vary μ in the range of 0.1 to 0.3 GeV, leading to practically unchanged scattering amplitudes and thus the same medium effects. We do not consider members of such a family of fits as different. The slight change in χ^2 corresponds to variation (in a certain range) of the parameters of terms proportional to p^2 in the tree amplitudes, thus changing the effective-range values. This is not surprising considering the rather large error bars on the measured cross sections. As a consequence, the parameters $s'_1, s'_2, t'_1, t'_2, t'_3, u_1, u_2$ are not very well determined allowing fits with different effective-range values. Our experience shows that all these fits lead to quite similar scattering amplitudes and predictions for in-medium mass shifts.

Our strategy in dealing with these fits is to accept only those which do not imply spurious (quasi)bound states (‘‘hyperdeuterons’’) near threshold. For example, a fit with the lowest χ^2 led to negative effective range in the spin-singlet Σ^+p channel, $r_{\Sigma^+p}^{(0)} = -2.32$ fm. Together with the corresponding scattering length $a_{\Sigma^+p}^{(0)} = 2.64$ fm it would imply [14] a bound state with binding energy of 3.3 MeV, which is known not to exist. Therefore we rejected this fit.

With $\chi^2 = 13.5$ we obtained a fit with reasonable values of the range parameters and ΛN scattering lengths close to values of model NSC97f in Ref. [12]. The corresponding set (denoted by A) of parameters is the following: $\mu = 0.15$ GeV, $s_1 = 1.00$, $s_2 = 1.78$, $t_1 = 1.21$, $t_2 = 3.43$, $t_3 = 1.87$, $s'_1 = -0.447$, $s'_2 = 1.82$, $t'_1 = -2.42$, $t'_2 = 1.05$, $t'_3 = 3.60$, $u_1 = -0.260$, and $u_2 = -0.0998$. The resulting cross sections are shown in Fig. 1. The calculated value of the capture ratio is $r_R = 0.4670$, the ΛN scattering lengths and range parameters are $a_{\Lambda N}^{(0)} = -2.50$ fm, $r_{\Lambda N}^{(0)} = 1.61$ fm, $a_{\Lambda N}^{(1)} = -1.78$ fm, $r_{\Lambda N}^{(1)} = 1.42$ fm. For $\Sigma^+p \rightarrow \Sigma^+p$ scattering we then obtain $a_{\Sigma^+p}^{(0)} = 0.55$ fm, $r_{\Sigma^+p}^{(0)} = 0.36$ fm, $a_{\Sigma^+p}^{(1)} = 0.94$ fm, $r_{\Sigma^+p}^{(1)} = 0.35$ fm. These values are quite different from those of model NSC97f.

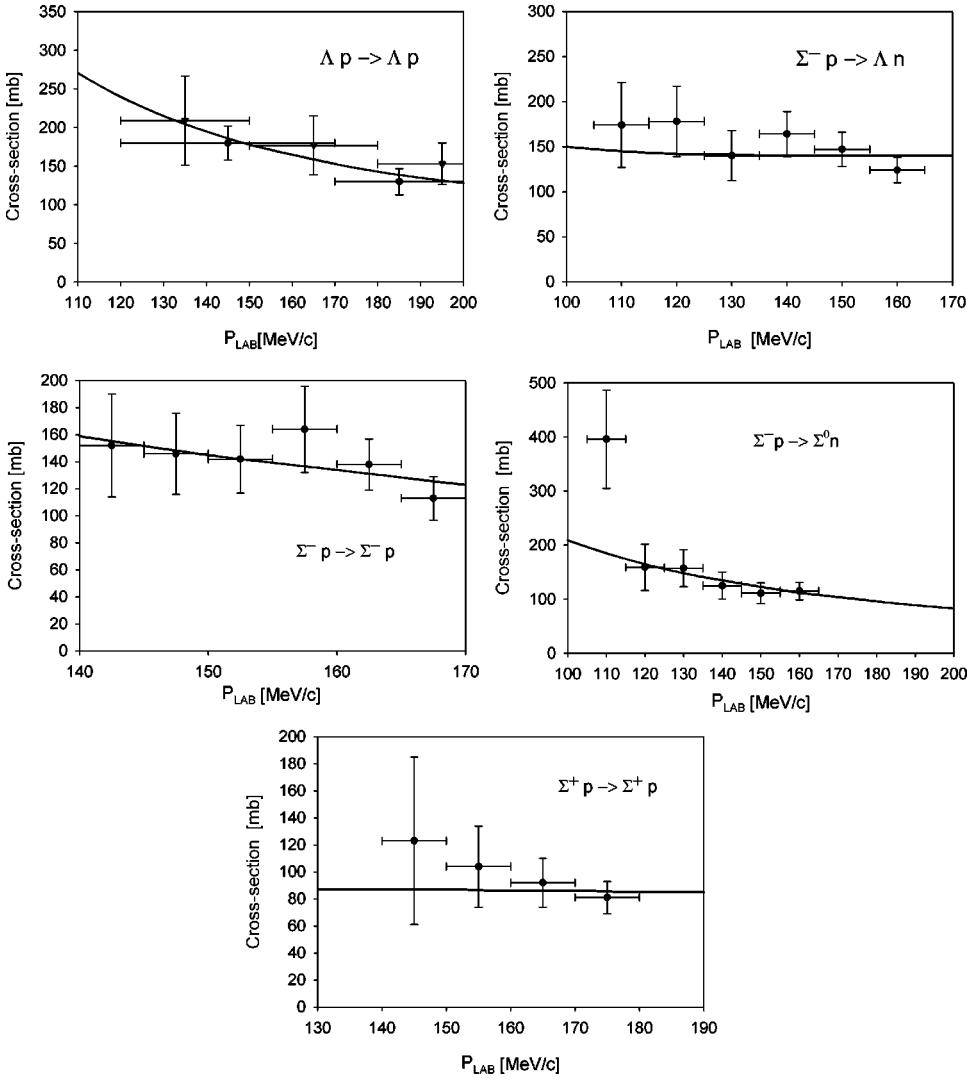


FIG. 1. Results of the fit (line) to YN cross sections with parameter set A.

Our results high-light one of the main problems with the available hyperon-nucleon scattering data (apart from the large error bars): the absence of truly low-energy cross sections. Figure 1 shows that the lowest hyperon (laboratory) momentum is larger than 100 MeV/c, which means that the reciprocal of the scattering length and the range term $\frac{1}{2}rp^2$ can be of the same order. This leads to results for the scattering lengths and effective ranges that are not unique. We mention that we could not obtain a satisfactory fit to the data with both Λ -nucleon and Σ^+ -proton scattering lengths being close to the values given in Ref. [12].

IV. HYPERON MASS SHIFTS IN THE NUCLEAR MEDIUM

Since we have dealt only with the low-momentum expansion of the hyperon-nucleon interaction, we can only consider hyperon self-energies in the nuclear medium in a low-density expansion [15]. A simple expression relates the in-medium mass shift (i.e., the self-energy at zero momentum) to the hyperon-nucleon scattering lengths [2], viz.

$$\Delta M_Y = \frac{2\pi}{M_r} \left[\left(\frac{a_{Yn}^{(0)}}{4} + \frac{3a_{Yn}^{(1)}}{4} \right) \rho_n + \left(\frac{a_{Yp}^{(0)}}{4} + \frac{3a_{Yp}^{(1)}}{4} \right) \rho_p \right], \quad (14)$$

where M_r is the reduced mass and ρ_n (ρ_p) is the neutron (proton) density.

A better approximation is obtained when one takes into account the Fermi motion of the nucleons, which amounts to integrating the momentum-dependent forward-scattering amplitude in the nucleon Fermi sea. In this case one has

$$\begin{aligned} \Delta M_Y &= -\frac{1}{4} \left[2 \int_0^{p_{F_n}} [\mathcal{A}_{Yn}^{(0)}(0, \vec{p}; 0, \vec{p}) + 3\mathcal{A}_{Yn}^{(1)}(0, \vec{p}; 0, \vec{p})] \frac{d^3p}{(2\pi)^3} \right. \\ &\quad \left. + 2 \int_0^{p_{F_p}} [\mathcal{A}_{Yp}^{(0)}(0, \vec{p}; 0, \vec{p}) + 3\mathcal{A}_{Yp}^{(1)}(0, \vec{p}; 0, \vec{p})] \frac{d^3p}{(2\pi)^3} \right], \quad (15) \end{aligned}$$

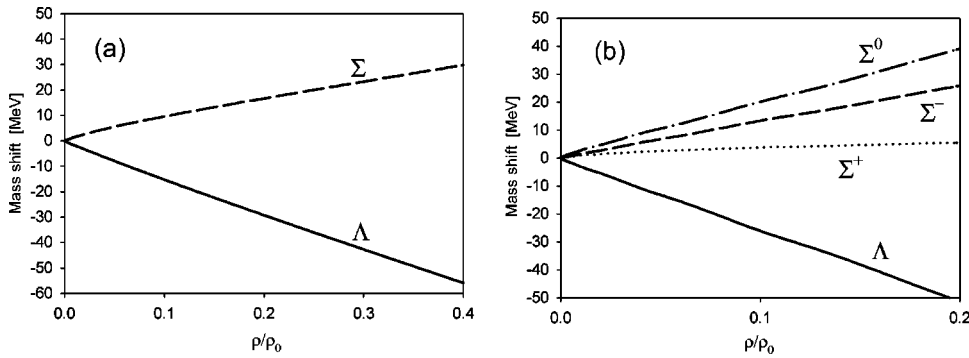


FIG. 2. Hyperon mass-shifts in isospin-symmetric matter (a) and neutron matter (b), calculated with parameter set A.

with $\mathcal{A}^{(0)}$ ($\mathcal{A}^{(1)}$) being the singlet (triplet) amplitude, \vec{p} is the nucleon momentum and that of the hyperon is zero.

Since our fits to cross sections extend only up to momenta of 200 MeV/c, that leads to a maximum density of $0.4\rho_0$ for the case of isospin-symmetric matter and $0.2\rho_0$ for neutron matter ($\rho_0 = 0.17 \text{ fm}^{-3}$ is the saturation density). Results for hyperon mass shifts for the parameter set A are shown in Fig. 2 for isospin-symmetric matter (a), and pure neutron matter (b).

The results for the Λ mass shift in Fig. 2(a) are similar to those obtained in Refs. [16–19] using the Brueckner-Hartree-Fock (BHF) method with the OBE potential from Ref. [20], except that there the linear behavior holds up to $0.2\rho_0$, after which nonlinear behavior, leading eventually to saturation, sets in. For the Σ mass shift the results differ, since in Ref. [16] a small mass decrease is found at small nucleon density. We mention that the hypertriton calculation [10] shows that the hyperon in ${}^3_\Lambda H$ is a Λ with probability greater than 95%, thus the behavior of the Σ in nuclear medium has a very small effect on the binding energy.

Results for neutron matter cannot be compared directly with those of the BHF method (and potentials used), since only larger densities were considered in Refs. [16–18], as well as in Ref. [21]. Low-density results [22] show linear behavior until about $0.2\rho_0$ and striking differences for different potentials. Mass shifts based on parameter set A, Fig. 2(b), show similar behavior to these BHF results [16–18,21], with the difference that the latter predict the Σ^0 curve below that of Σ^- . We mention that in this case, because of isospin-symmetry violation in the neutron matter, the nondiagonal mass shift $\Delta M_{\Lambda\Sigma}$ is nonzero and quite large for our param-

eter values, leading to strong repulsion of the Λ and Σ^0 curves. Without this repulsion we would recover the “natural” ordering (in increasing mass shift) of the Σ^+ , Σ^0 , Σ^- curves. Also, the BHF calculations seem to prefer a mass decrease for the Σ hyperons (except for Σ^- and, depending on the potential, also for Σ^0), compared to our repulsion.

We conclude that due to the scarce scattering data the predicted hyperon mass shifts in the nuclear medium are somewhat uncertain, but the uncertainty can be partly eliminated using conclusions from the existence of the hypertriton bound state and imposing a constraint of reasonable effective-range values, thus avoiding spurious hyperon-nucleon bound states. Computations in the BHF scheme provide more reliable results for larger densities, but they suffer from serious ambiguities stemming from the use of different potentials, all of which describe the scattering data equally well.

ACKNOWLEDGMENTS

We acknowledge useful discussions with U. van Kolck and T. Motoba, as well as helpful correspondence with H.-J. Schulze and Y. Yamamoto. This research was supported in part by the Hungarian Research Foundation (OTKA) Grant No. T030855 and by the NWO-OTKA Grant No. 834012. The research of R.G.E.T. was made possible by funds from the Royal Netherlands Academy of Arts and Sciences. That of A.E.L.D. is part of the research program of the “Stichting voor Fundamenteel Onderzoek der Materie” (FOM) with financial support from the “Nederlandse Organisatie voor Wetenschappelijk Onderzoek” (NWO).

- [1] J. Dabrowski, Phys. Rev. C **60**, 025205 (1999).
- [2] M.J. Savage and M.B. Wise, Phys. Rev. D **53**, 349 (1996).
- [3] U. van Kolck, Prog. Part. Nucl. Phys. **43**, 337 (1999).
- [4] S.R. Beane, P.F. Bedaque, W.C. Haxton, D.R. Phillips, and M.J. Savage, nucl-th/0008064.
- [5] D.B. Kaplan, M.J. Savage, and M.B. Wise, Nucl. Phys. **B534**, 329 (1998).
- [6] J. Gegelia, Phys. Lett. B **463**, 133 (1999).
- [7] T. Mehen and I.W. Stewart, Phys. Lett. B **445**, 378 (1999).
- [8] U. van Kolck, in *Mainz 1997, Chiral Dynamics: Theory and Experiment*, edited by A.M. Bernstein, D. Drechsel, and T.

- Walcher (Springer Verlag, Berlin, 1998); Nucl. Phys. **A645**, 273 (1999).
- [9] S. Fleming, T. Mehen, and I.W. Stewart, Phys. Rev. C **61**, 044005 (2000); Nucl. Phys. **A677**, 323 (2000).
- [10] K. Miyagawa, H. Kamada, W. Glöckle, and V. Stoks, Phys. Rev. C **51**, 2905 (1995).
- [11] C.B. Dover and H. Feshbach, Ann. Phys. (N.Y.) **198**, 321 (1990).
- [12] Th.A. Rijken, V.G.J. Stoks, and Y. Yamamoto, Phys. Rev. C **59**, 21 (1999).
- [13] J.J. de Swart, M.M. Nagels, T.A. Rijken, and P.A. Verhoeven,

- Springer Tracts Mod. Phys. **60**, 138 (1971).
- [14] M. Lutz, Nucl. Phys. **A677**, 241 (2000).
- [15] C.B. Dover, J. Hüfner, and R.H. Lemmer, Ann. Phys. (N.Y.) **66**, 248 (1971).
- [16] H.-J. Schulze, M. Baldo, U. Lombardo, J. Cugnon, and A. Lejeune, Phys. Rev. C **57**, 704 (1998).
- [17] H.-J. Schulze, A. Lejeune, J. Cugnon, M. Baldo, and U. Lombardo, Phys. Lett. B **355**, 21 (1995).
- [18] M. Baldo, G.F. Burgio, and H.-J. Schulze, Phys. Rev. C **58**, 3688 (1998).
- [19] H.-J. Schulze (private communication).
- [20] P.M.M. Maessen, Th.A. Rijken, and J.J. de Swart, Phys. Rev. C **40**, 2226 (1989); R.G.E. Timmermans, Th.A. Rijken, and J.J. de Swart, Phys. Rev. D **45**, 2288 (1992).
- [21] Y. Yamamoto, S. Nishizaki, and T. Takatsuka, Prog. Theor. Phys. **103**, 981 (2000).
- [22] Toshio Motoba (private communication).